Mecánica Computacional Vol. XXIII, pp. 2443-2458
G.Buscaglia, E.Dari, O.Zamonsky (Eds.)
Bariloche, Argentina, November 2004

A SIMPLIFIED MODEL FOR HEAT TREATMENT SIMULATION

José Risso[*], Alberto Cardona[*] and Andres Anca[*]

[*] CIMEC - INTEC
(UNL / Conicet)
Güemes 3450, (3000) Santa Fe, Argentina
e-mail: acardona@intec.unl.edu.ar

Key words: Heat Treatment, Thermal Stresses, Solid Mechanics

Abstract. *This work presents a simplified model to predict strain and stresses produced during heat treatment of ferrous alloys, using the finite element method. From a computational point of view, this problem requires coupled thermal-metallurgical-mechanical analysis, modeled as non-stationary and nonlinear processes. Calculation of metallurgical properties is coupled directly with thermal analysis, because thermal properties depend on microstructural composition. Metallurgical transformations occurring during the process are important in the development of internal stresses and distortions, because they change mechanical properties of the metal, but also involve specific volume changes that are coupled to thermal dilatations. The microstructures formed during heat treatment depend on alloy composition, temperatures and cooling rate, as can be observed in TTT or CCT diagrams. For a given material, their properties could be considered as functions of temperature and microstructural composition and, in a second analysis, as functions of temperature and time. Taking into account the difficulties to obtain material parameters to model accurately their properties with more sophisticated models, a piecewise linear model is proposed. A numerical example applied to a real case is presented.*

1 INTRODUCTION

Heat treatment of metallic alloys is a complex thermomechanical process involving solid state metallurgical transformations that change both thermal and mechanical properties of materials.

This process is widely used in industrial applications, to release internal stresses, reduce fragility, improve machinability or modify properties like hardness or strength, to satisfy the requirements of a definite application. However, heat treatment can cause, during or after them, undesirable strains and stresses, and also cracking of parts. This fact must be taken into account when designing the heating and cooling sequence of the process.

Numerical simulation of heat treatment was subject of many research works. Some of them focused on thermal and mechanical analysis of the process [3,4,12], while the others focused on aspects of material modeling [1,8,9,13].

Material models with the ability to account for variations in thermal and mechanical properties due to temperature and metallurgical structure changes are a key point to simulate accurately the thermomechanical evolution of parts subjected to heat treatment. Several models describe material properties as functions of alloy composition, temperature and microstructure. Other models describe the evolution of microstructure as a function of alloy composition and cooling time, reproducing TTT or CCT diagrams for different alloys and chemical compositions.

Even though advanced material models are very useful to cover a broad range of chemical compositions for some well-known alloys (carbon steels, low-alloy steels, austenitic stainless steels), their efficacy for other alloys is very limited because of the difficulty to obtain all the coefficients needed to represent accurately their behavior (e.g. for high-alloy white iron).

In this work, we follow an alternative simplified way to simulate heat treatment, using material properties defined as functions of time and temperature, obtained by merging TTT/CCT diagrams with curves of dependency of thermomechanical properties with temperature. Simulations were done using the commercial finite element software SAMCEF.

Section 2.1 describes the numerical model used to simulate thermomechanical processes in heat treatment of ferrous metals. In section 2.2, a description of the proposed material model is given. Section 3 presents an application of this model to simulation of heat treatment of centrifugally cast, three-layer, Hi-Chrome work rolls, commonly used in steel mills.

2 NUMERICAL MODEL

2.1 Thermomechanical model

Numerical analysis of heat treatment processes can be made by modeling the time evolution of two coupled problems:

1) a thermal one, that involves heating and cooling of parts and must take into account variations in material properties (thermal conductivity and enthalpy) due to temperature and microstructural transformations, and also heat releasing/absorption

(related with latent heat) during metallurgical transformations.

2) a mechanical one, to predict stresses and strains generated by thermal expansion/contraction produced by temperature changes and also by metallurgical phase transformations.

The thermal problem is non-linear, because thermal parameters are dependent of temperature. The mechanical problem is also non-linear, because thermal and transformation-induced strains often generate plastic deformations.

In absence of very strong mechanical perturbations that could induce metallurgical transformations (e.g. transformation of retained austenite to martensite, induced by stresses generated by external loads), mechanical phenomena do not affect thermal properties. This fact releases the dependency of the thermal model on mechanical variables, and enables us to perform an uncoupled thermal analysis, followed by a mechanical analysis that takes thermal results as inputs.

The dependence of the thermal problem on metallurgical transformations is simulated with an enthalpy model that takes into account heat capacity of metal, and latent heat exchange occurring during phase changes.

The differential equation describing the problem is:

$$\rho_{(T)} \frac{\partial H_{(T,m)}}{\partial t} - \nabla(k_{(T,m)} \nabla T) = 0 \tag{1}$$

where ρ is the density, H the enthalpy, t is the time, k the conductivity, T the temperature and m accounts for the dependency of material parameters on microstructure.

Convective boundary conditions are applied on the external surface of the roll:

$$-k_{(T,m)} \nabla T \cdot \mathbf{n} = h\ (T - T_b) \tag{2}$$

where $\mathbf{n}$ is the outer normal vector to the external surface, h is the film coefficient and T_b is the bulk (ambient) temperature.

The relationship between capacity and enthalpy in the presence of phase change is given by the following expression (assuming the same density for both phases) :

$$\rho_{(T)} H_{(T,m)} = \int_A^B \rho_{(T)} c_{eff\,(T,m)} dT = \int_A^{epc} \varphi_{1(T)} \rho_{(T)} c_{1(T)} dT + \rho_{(T)} L_{pc} + \int_{spc}^B \varphi_{2(T)} \rho_{(T)} c_{2(T)} dT \tag{3}$$

where c_{eff} is the effective (apparent) heat capacity, c_1 and c_2 are the specific heats for different microstructures, φ_1 and φ_2 are proportions of initial and final microstructural components, L_{pc} is the latent heat necessary for a phase change, *spc* is the initial temperature of phase change and *epc* the temperature at the end of phase change.

The dependence of the mechanical properties on material microstructure is simulated using material models that account for variations in metallurgical constituents with time. The thermal dependence of the mechanical problem is modeled using a thermal field calculated in

the thermal simulation and given as input to evaluate the mechanical properties for the mechanical analysis and to compute the strains.

In the mechanical simulation, we use an elastoplastic model in which the stresses are calculated as:

$$\boldsymbol{\sigma} = \mathbf{C}_{(T,\varepsilon_p,m)}\boldsymbol{\varepsilon}_e = \mathbf{C}_{(T,\varepsilon_p,m)}\left(\boldsymbol{\varepsilon} - \boldsymbol{\varepsilon}_p - \boldsymbol{\varepsilon}_t\right) \tag{4}$$

where $\boldsymbol{\sigma}$ and $\boldsymbol{\varepsilon}$ are stress and strain vectors, $\mathbf{C}$ is the constitutive tensor, $\boldsymbol{\varepsilon}_\mathbf{e}$ is the elastic strain, $\boldsymbol{\varepsilon}_\mathbf{p}$ is the plastic strain and $\boldsymbol{\varepsilon}_\mathbf{t}$ is the thermal strain.

The thermal strain is calculated as:

$$\boldsymbol{\varepsilon}_t = \begin{pmatrix} \alpha_{(T)} \\ \alpha_{(T)} \\ \alpha_{(T)} \\ 0 \\ 0 \\ 0 \end{pmatrix} \left(T - T_{ref}\right) \tag{5}$$

where α is the thermal dilatation coefficient and T_{ref} is the reference (zero strain) temperature.

The stress field must satisfy a yield criterion (in this case, the isotropic Von Mises criterion):

$$\sigma_{eq}(\boldsymbol{\sigma}) = \sqrt{\frac{1}{2}\left(\left(\sigma_x - \sigma_y\right)^2 + \left(\sigma_y - \sigma_z\right)^2 + \left(\sigma_z - \sigma_y\right)^2 + 6\left(\tau_{xy}^2 + \tau_{yz}^2 + \tau_{zx}^2\right)\right)} \leq Y_{(T,\varepsilon_{eq})} \tag{6}$$

Since the limit stress Y is a function of the equivalent plastic strain (ε_{eq}) and temperature, the model can take into account different material hardening behaviors at different temperatures.

2.2 Material model

Most material properties are a function of temperature and microstructure, and therefore they have indirect dependency on variables defining material microstructure, like time and maximal heating/cooling temperature .

In austenitizing processes (heating), the microstructure is modeled as a function of temperature. In quenching processes (cooling), the microstructure is a function of temperature and time. In tempering processes (heating and cooling), the microstructure is considered as a function of only temperature.

Then, for the whole process, we can formulate any general property μ, as dependent on temperature and time, as follows:

$$\mu = \mu_{(T, m_{(T,t)})} = \mu_{(T,t)} \tag{7}$$

To define material parameters, we first construct a map of microstructure as a function of temperature and time, using data about heating and cooling periods, and isothermal (TTT) or continuous cooling (CCT) diagrams for the quenching cooling interval, as shown in figure 1.

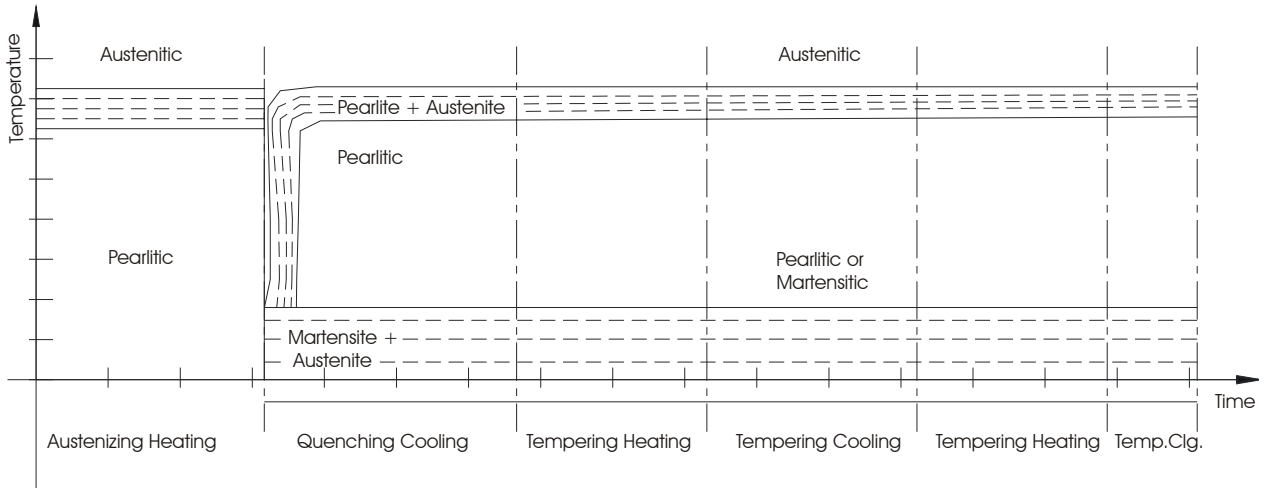

Figure 1. Temperature – time - transformation approximation.

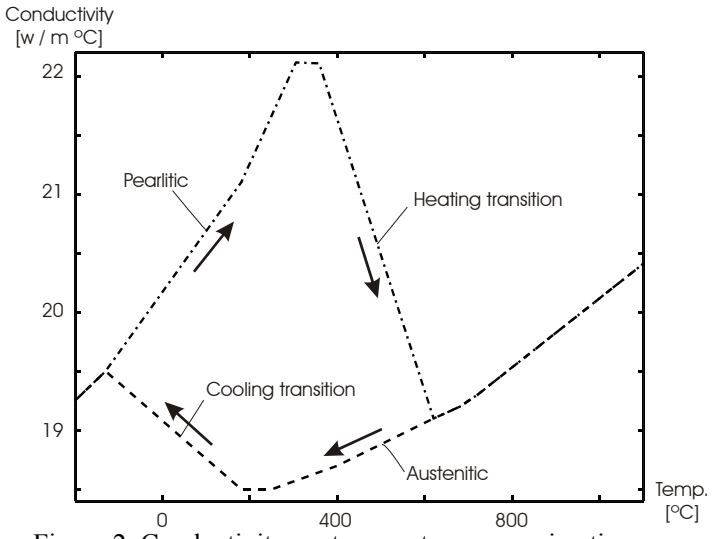

Figure 2. Conductivity vs. temperature approximation.

Then, for every definite material microstructure (i.e.: austenitic, pearlitic, martensitic), we define the value of every property as a function of temperature. Figure 2 is an example for conductivity during the heating process.

Finally, by combining the map of microstructure as a function of temperature and time, with the curves of temperature dependence of the considered property, and by using the rule

of mixtures for regions with mixed structure (e.g. austenite + pearlite), a map of the property as a function of temperature and time (continuous piecewise linear approximation) can be built, as shown in figure 3.

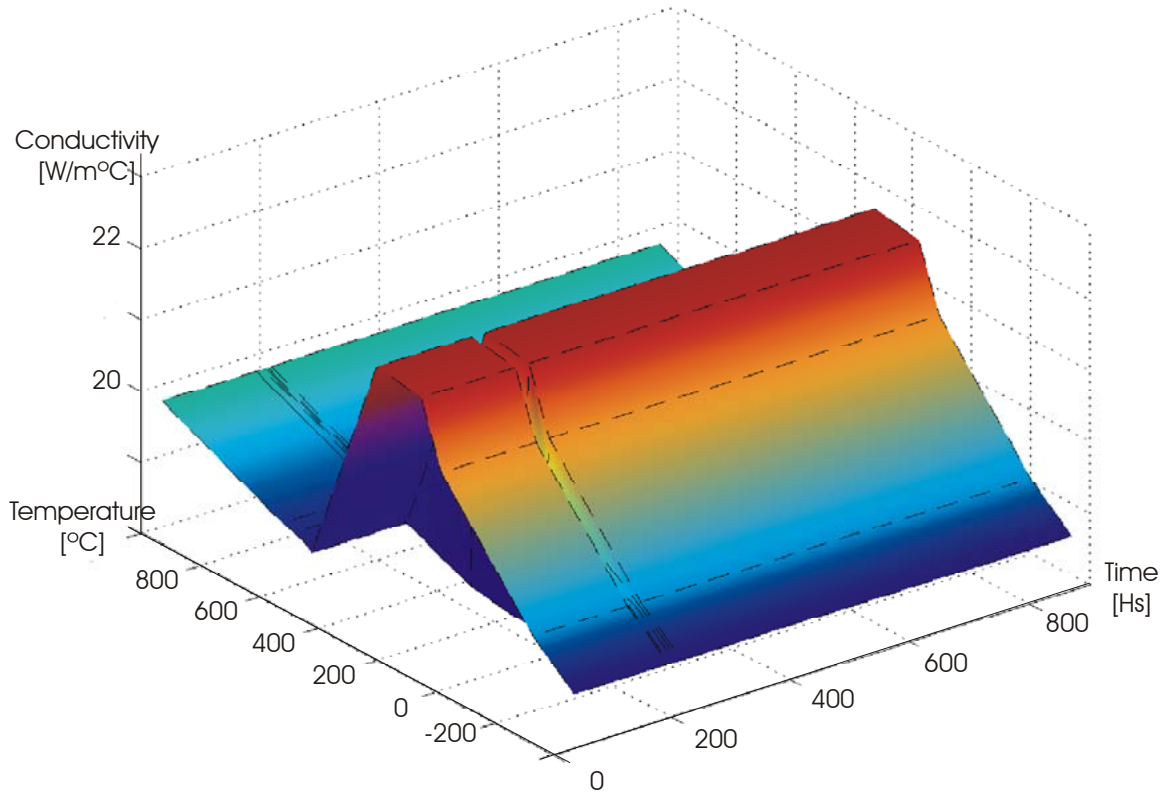

Figure 3. Conductivity vs. temperature and time diagram.

In this work, we used the commercial finite element code SAMCEF V10.1, in which material properties can be defined as functions of temperature and time. Using a standard material model, special care must be taken to adapt the map of microstructure as a function of temperature and time to the real quenching cooling process, thus avoiding reversions in austenite-pearlite and austenite-martensite transformations. An improvement will be the development of a model with the ability to track microstructural evolution and avoid numerical reversion of physically irreversible phase changes. This work is in progress and being implemented in our object-oriented finite element code OOFELIE.

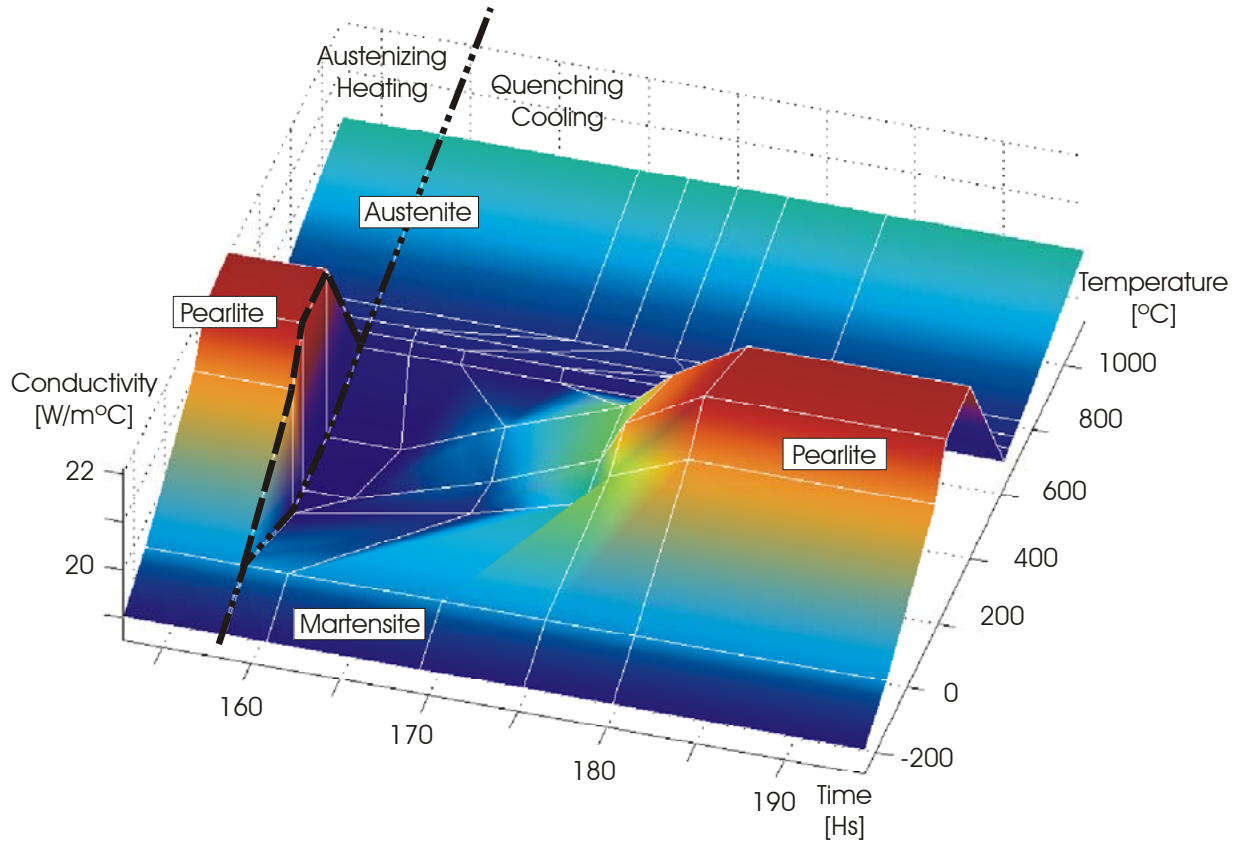

Figure 4: Conductivity vs. time and temperature diagram – Detail in the quenching cooling zone

In the thermal analysis, the material parameters are enthalpy and thermal conductivity. In the mechanical analysis, the material parameters are Young (elastic) modulus, Poisson coefficient, thermal expansion coefficient, and yield stress. All of them are modeled following the above mentioned procedure.

3 APPLICATION CASE

3.1 Problem description

Hi-Chrome work rolls have an exterior layer (shell) of Hi-Chrome white iron, an intermediate layer of low-alloy iron, and a core of spheroidal graphite iron. The first two layers are casted centrifugally, and then the core is poured statically. Typical as-cast dimensions are shown in figure 5.

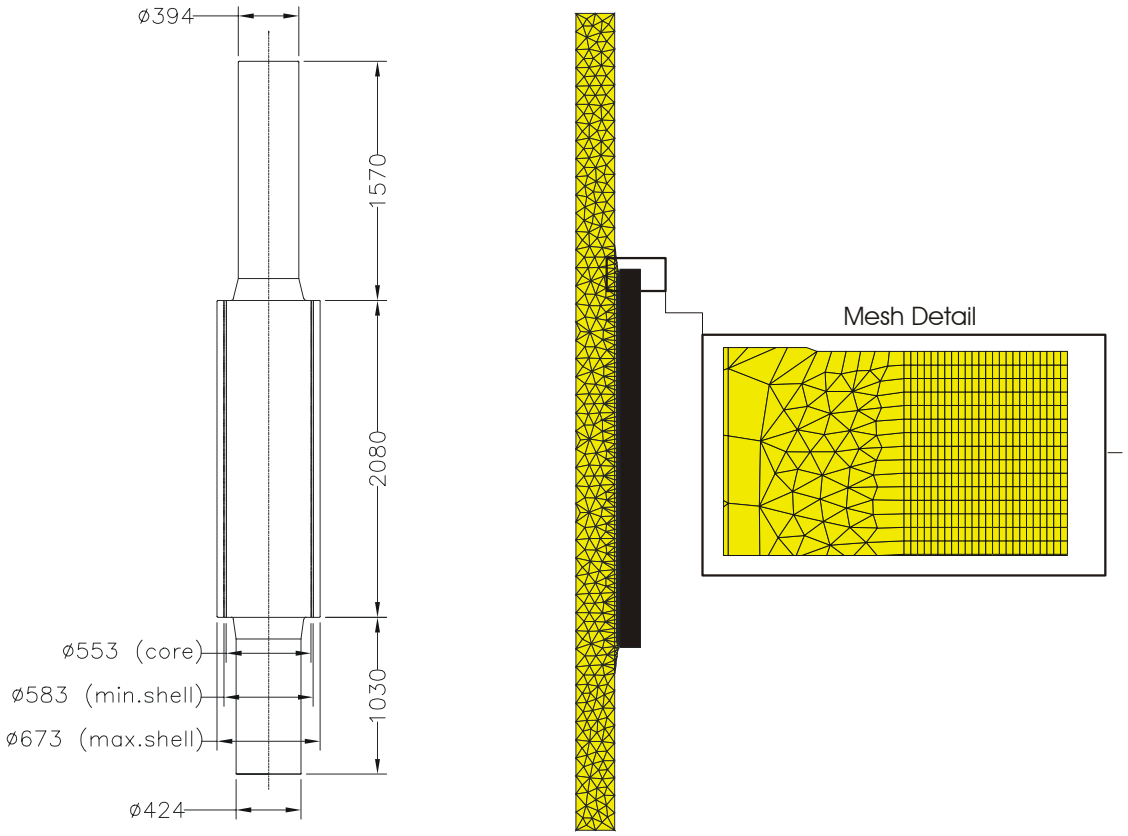

Figure 5. a) Work roll general dimensions. b) FEM Mesh .

After casting, rolls are heated to 1020 ºC (with complete austenitization), then they are quenched cooled in air to room temperature, and finally subjected to two tempering processes at 480 ºC and 540 ºC with air cooling to room temperature. This process requires special care to avoid defects as cracking near the edges of the barrel.

By ignoring small circumferential temperature differences, and small bending stresses generated by the horizontal mounting of cylinders, the problem can be modeled as an axisymmetrical one. The finite element mesh is shown in figure 5.

Convective boundary conditions were modeled on the external surface of the roll. Film coefficients ranging from 5 [W/(m^{2}ºC)] to 40 [W/(m^{2}ºC)] were used in the different stages of heating and cooling, depending on the agitation of surrounding air.

3.2 Shell material data (Hi-Chrome white cast iron)

A TTT diagram for a similar alloy was used to determine position of pearlitic nose [5]. The cooling behavior of the shell material was determined using a CCT diagram for a Hi-Cr white iron without Ni [7], with a correction of the transformation time to take into account the influence of Ni and Mo, as suggested by Laird et al. [10]. A plot of the used diagram is shown in figure 6.

Thermal conductivity as a function of temperature and microstructure was taken from data

for High-Alloy white iron [5,14].

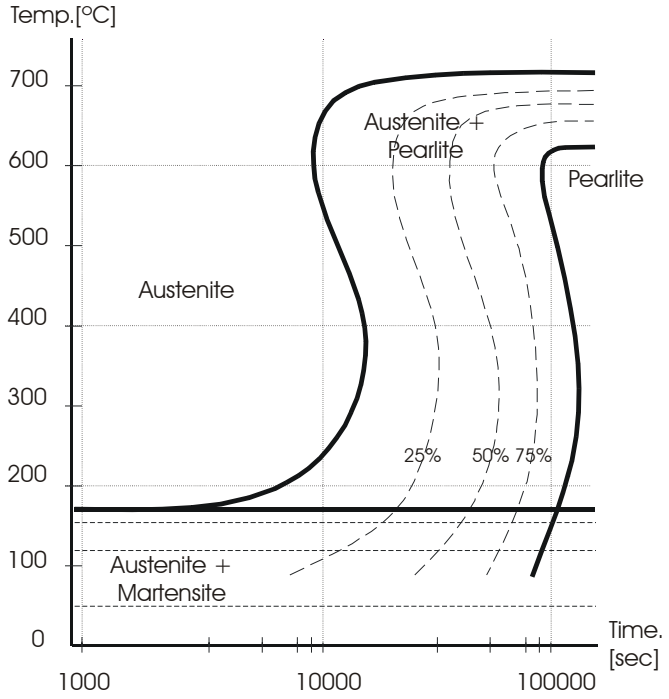

Figure 6. Temperature – Time - Transformation diagram for shell material.

Enthalpy values were calculated using 0ºK as a reference temperature and integrating effective thermal capacity data [5,14] along the temperature range covered in the process. In order to calculate thermal strains, a secant thermal expansion coefficient averaged from values found in bibliography [7,14] was used.

The elastic modulus as a function of temperature and chemical composition was obtained from data published by Belyakova et al. [2,10].

Poisson coefficient was supposed constant and equal to 0.28.

Since no data about yield stress dependence on temperature could be found, we supposed a variation based on the room temperature yield stress with thermal dependency of ultimate tensile stress for Hi-Cr white iron [10]. An isotropic hardening law was used.

3.3 Layer and core material data (Gray and SG cast iron)

A TTT diagram for Ni-Mo ductile iron [6] was used to define the microstructure as a function of time and temperature in quenching cooling. A plot of this diagram is shown in figure 7.

Thermal conductivity and enthalpy (obtained integrating apparent thermal capacity) as a function of heating and cooling temperature was taken from data published by Auburn University researchers [15].

In order to calculate thermal strains, a secant thermal expansion coefficient was calculated from tables of total thermal expansion in heating and cooling, published by the Auburn

Solidification Design Center [15].

The elastic modulus as a function of temperature was extrapolated from values at room temperature [5] and thermal dependency of this parameter for pearlitic steels.

Poisson coefficient was supposed constant and equal to 0.26.

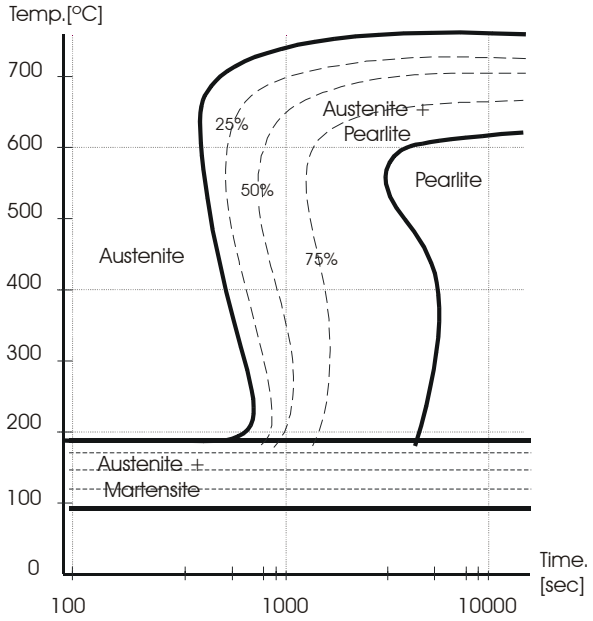

Figure 7. Temperature – Time - Transformation diagram for core material.

Yield stress dependence on temperature was taken from tables for SG iron of similar composition [11].

3.4 Results

In figure 8, a comparison between calculated (continuous line) and measured (dashed line) temperatures at the midpoint of the barrel surface is shown. The agreement between curves is found quite acceptable for the purposes of the analysis.

The largest differences between temperatures in different points of the roll are found at the initial stage of quenching cooling. Figure 9 shows a detail of these differences between points located in the surface of the barrel (P1, P4) and others situated in the zones of transition between layers of different materials.

In figures 10 to 17, the evolution of temperatures, principal stresses and equivalent plastic deformations near the corner are shown. The time instants of these plots along the complete heat treatment are referred by letters (A) to (H) in figure 8.

Temperature plots show very small differences between temperatures in different sectors of the roll during heating processes. Even during cooling processes with very high variations in time, the maximum temperature differences at a given time instant are below 200ºC. The computed temperature space gradients (radial) were also relatively small.

During the austenitizing heating, axial stresses in the shell are tensile stresses. However, as

plastic deformations occur during heating, in the quenching cooling and in the tempering processes axial stresses in the shell are compressive.

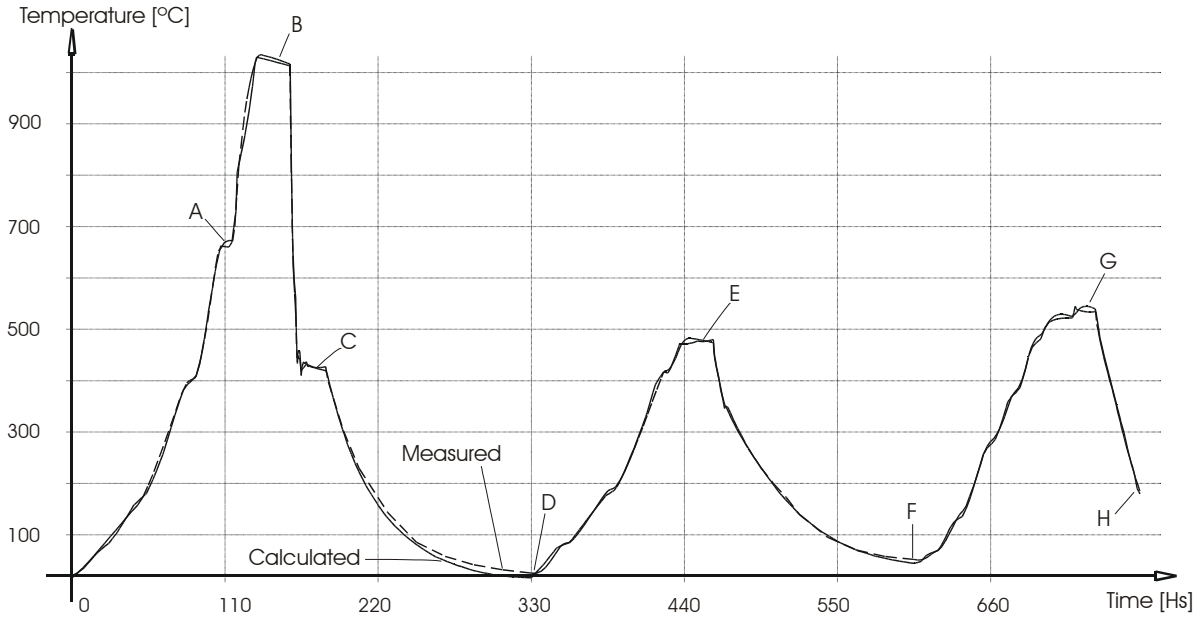

Figure 8. Comparison between calculated and measured temperatures in barrel midpoint.

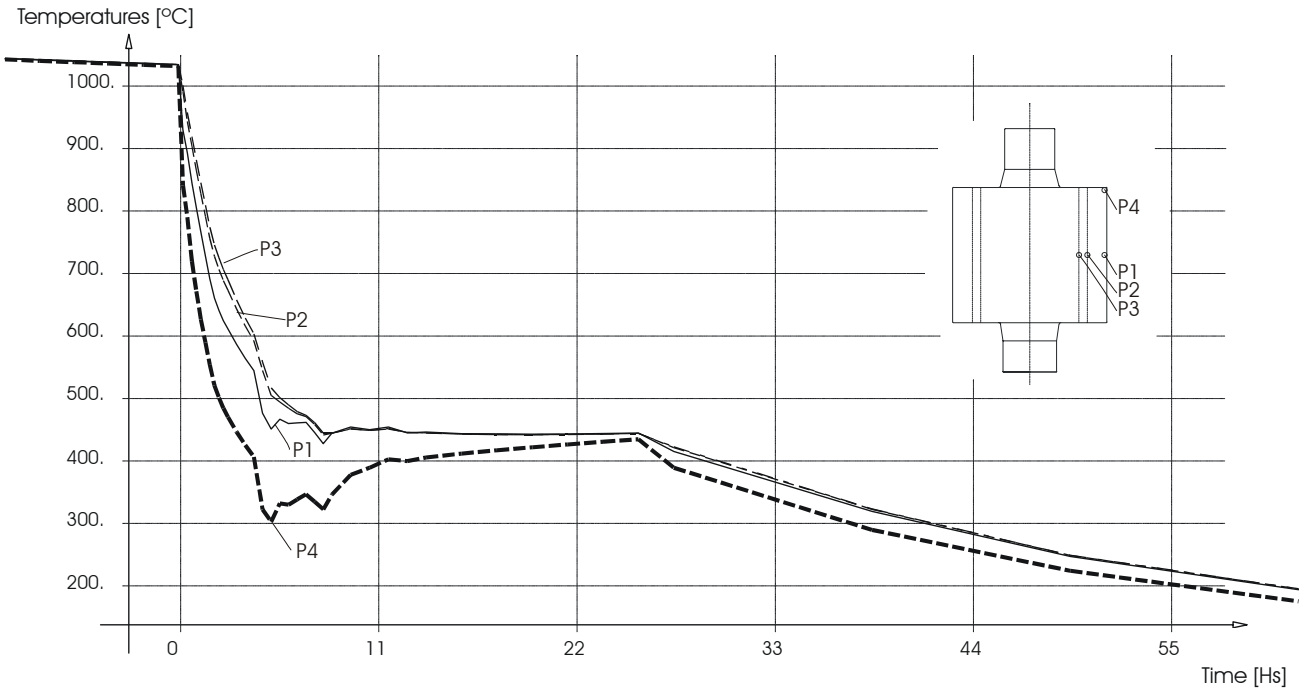

Figure 9: Temperature evolution in quenching cooling

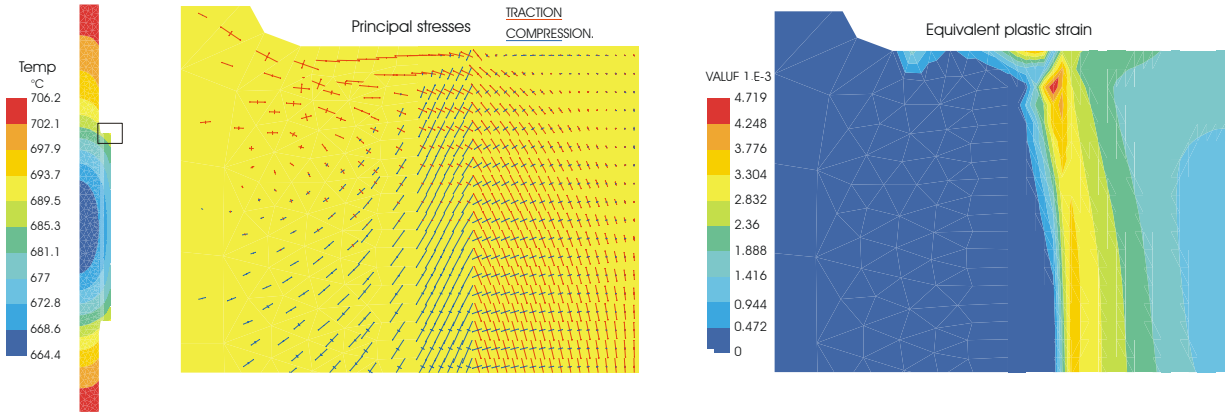

Figure 10: Intermediate point (A) of austenitizing heating (110 hs)

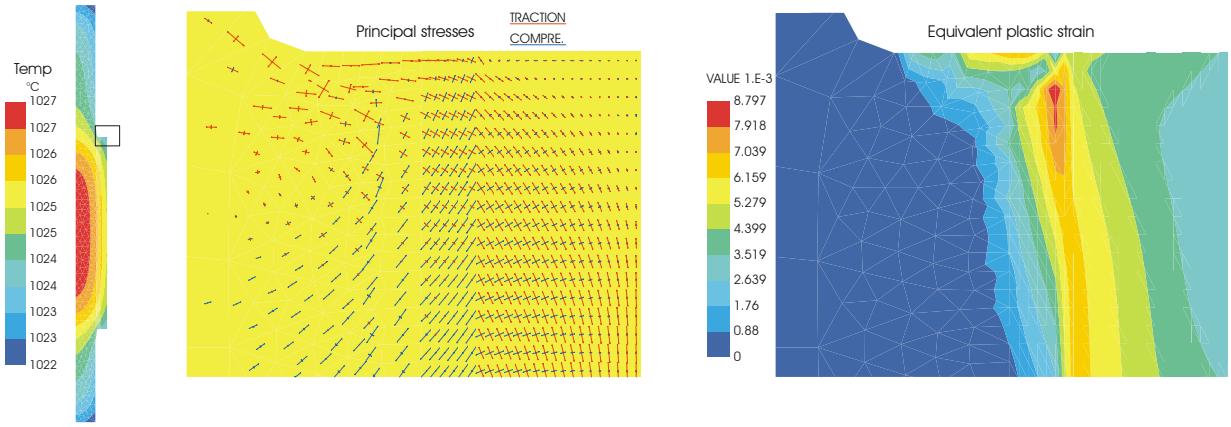

Figure 11: End (B) of austenitizing heating (156 hs)

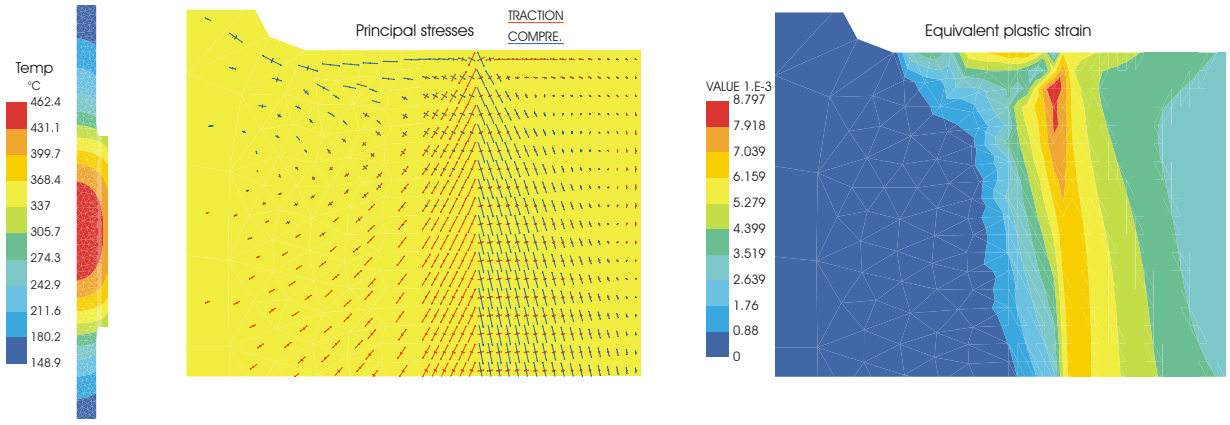

Figure 12: Intermediate point (C) of quenching cooling (166 hs)

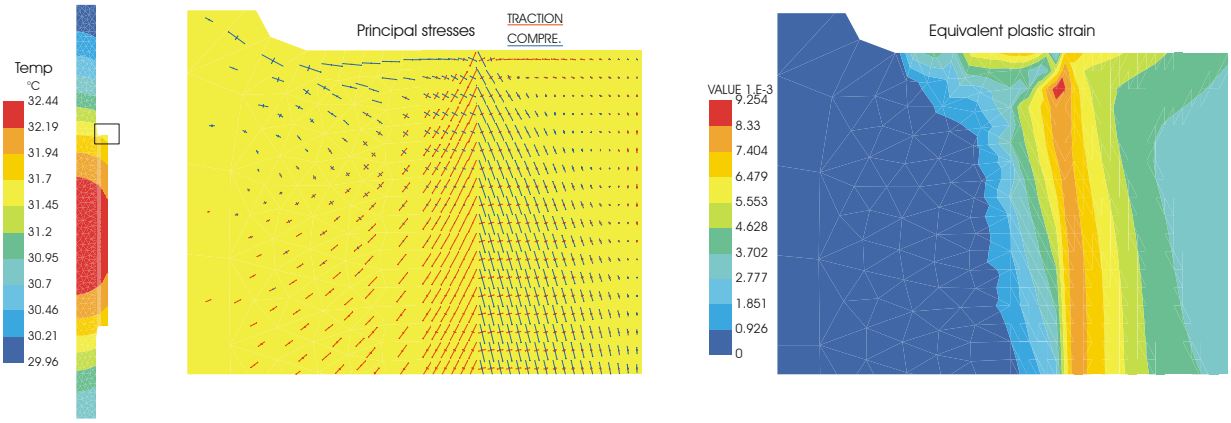

Figure 13: End (D) of quenching cooling (332 hs)

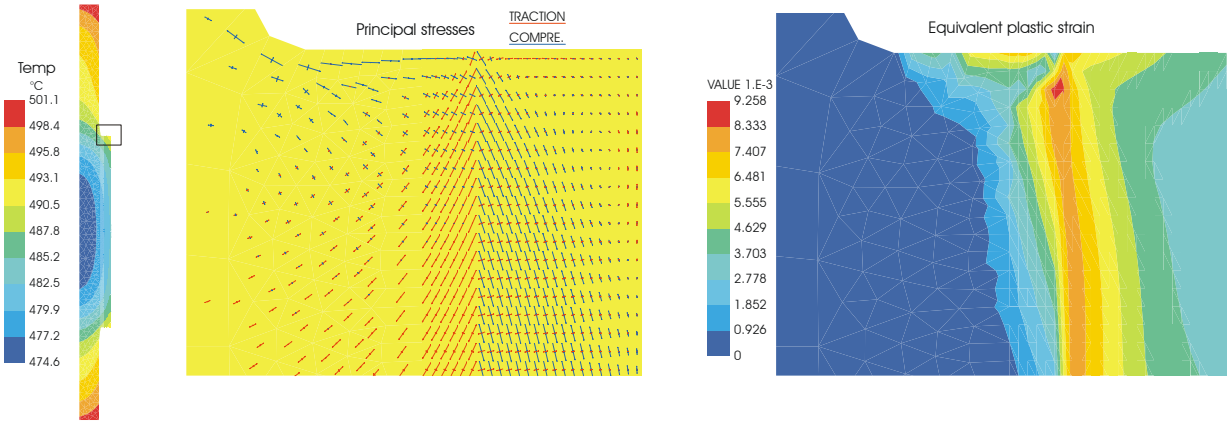

Figure 14: End (E) of first tempering heating (444 hs)

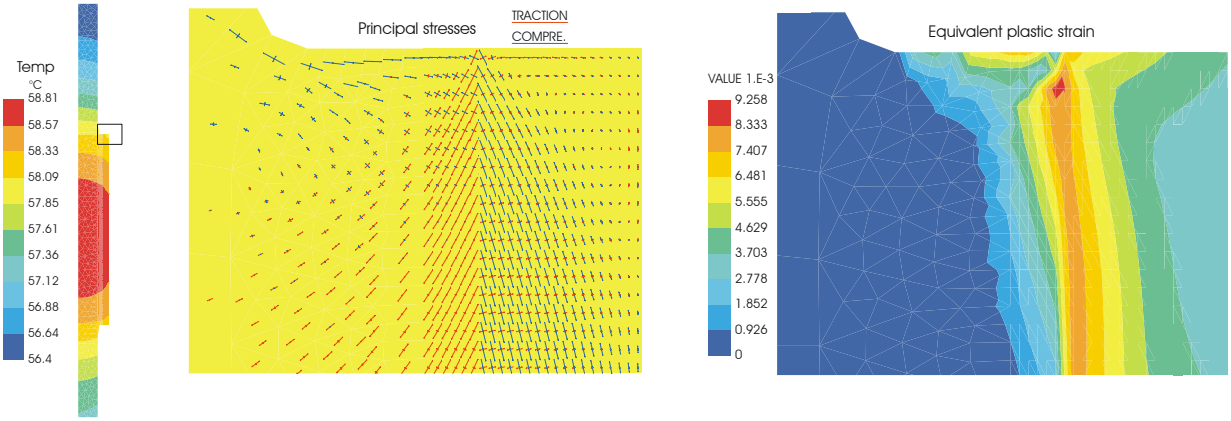

Figure 15: End (F) of first tempering cooling (609 hs)

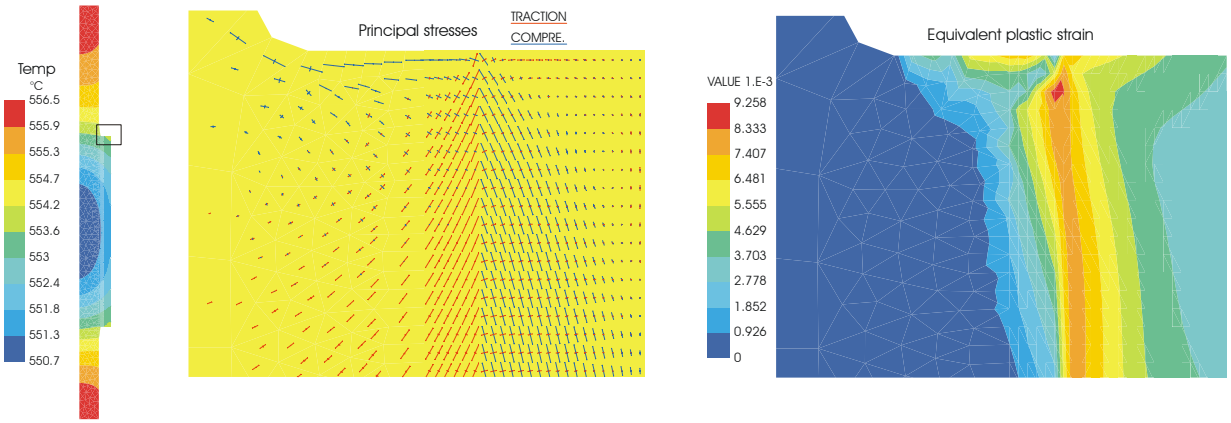

Figure 16: End (G) of second tempering heating (736 hs)

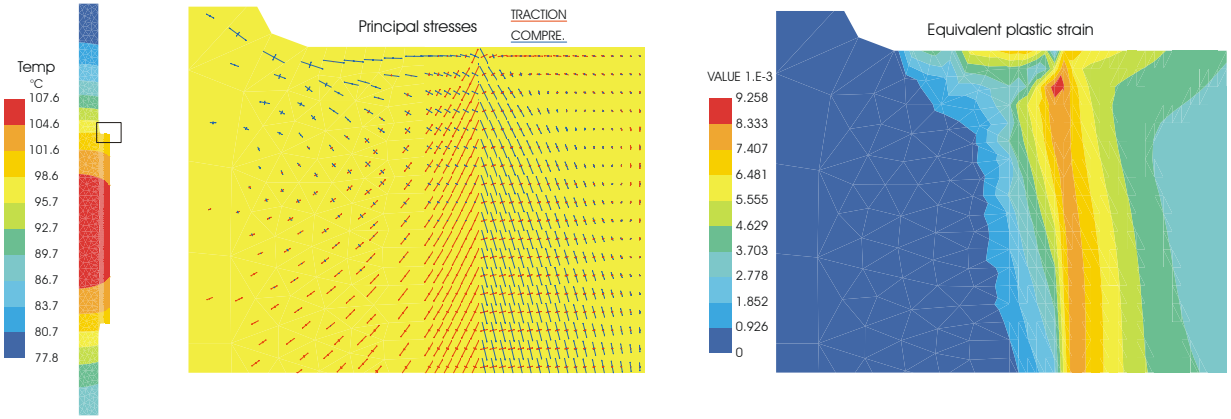

Figure 17: End (H) of second tempering cooling (792 hs)

Figure 18 shows the evolution of equivalent plastic strains in different points near the barrel corner.

Most of the inelastic deformations occur during the second half of the austenitizing heating process and during the quenching cooling, as shown in equivalent plastic strain plots. No evident increment of plastic strains is found during tempering processes. However, this result could be caused by the lack of information about percentages of retained austenite after quenching cooling and transformations of retained austenite during tempering.

The magnitude of inelastic strains found near the interface between shell and intermediate layers, close to 1%, are significative, specially taking into account the brittle nature of Hi-Chrome White iron.

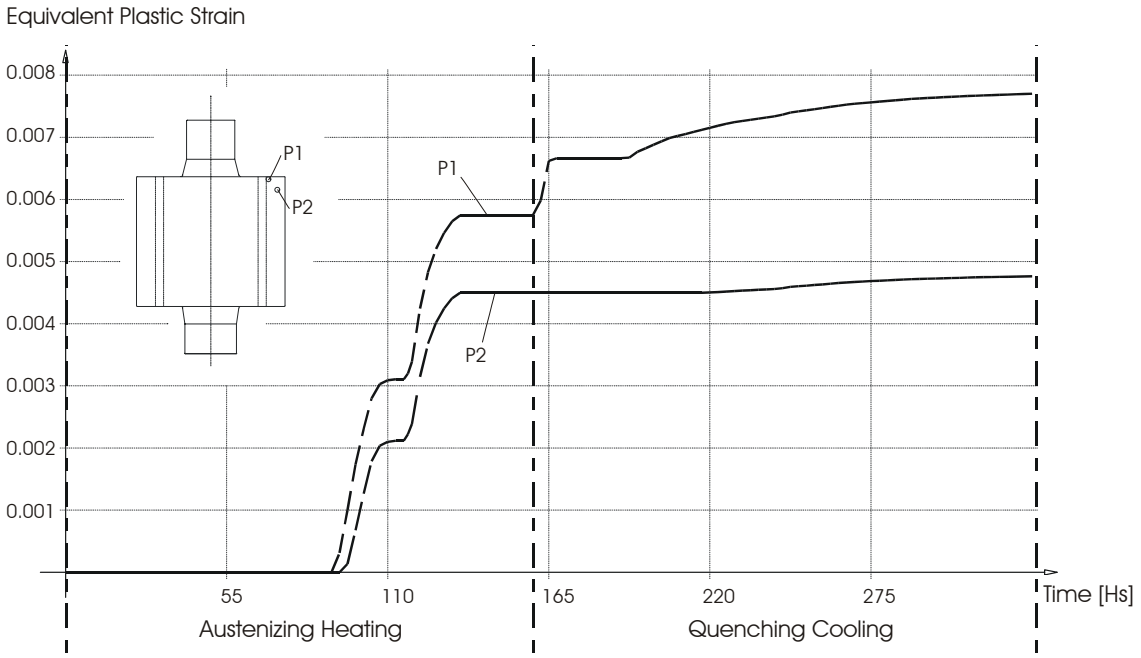

Figure 18: Evolution of equivalent plastic strain

4 CONCLUSIONS AND FUTURE WORK

A simplified model developed to simulate heat treatment of metals was presented.

The approximation used to model the thermomechanical variables was found to be useful in this case, for which material parameters are very scattered and difficult to be obtained.

Although the definition of material parameters is laborious, this type of parameterization permits to make an initial analysis with a minimal amount of data. The analysis may be refined later on, especially in those regions of the temperature-time-transformation diagram where the heating and cooling trajectory curves are passing.

The main drawbacks found are the inability of the model to prevent reverse (pearlite or bainite to austenite) transformations during quenching cooling, and to predict the microstructural composition of the metal after quenching cooling. These drawbacks will be solved with a new material model which is being implemented and keeps track of microstructural composition during the analysis.

Referring to the analysis of work rolls, these preliminary results show significant plastic deformations in the critical zone of the barrel. Most of them occur during the quenching cooling, and not during tempering. We think this result may be influenced by the lack of information about the behavior of retained austenite.

Finally, we should say that results may be improved by using an initial stress field computed with an analysis of solidification after casting, with development of stresses, and also by using data about evolution of retained austenite in the shell material.

5 REFERENCES

[1] Alberg H. "Material Modeling for Simulation of Heat Treatment". *Licentiate Thesis*, Lulea University of Technology (2003).
[2] Belyakova P.E. "Thermophysical Properties of Wear-Resisting Cast Irons". *Metallovediene I Termicheskaya Obrabotka Metallov.* (1975).
[3] Bergheau J.M. "Contribution of Numerical Simulation to the Analysis of Heat Treatment and Surface Hardening Processes". *Proc.of ASM Heat Treatment Conference'98* (1998).
[4] Berglund D. "Simulation of Welding and Stress Relief Heat Treatment in Development of Aerospace Components". *Licentiate Thesis*, Lulea University of Technology (2001).
[5] Betts W. Personal communication (2004).
[6] Boyer H.(ed.) *Atlas of Isothermal Transformations and Cooling Transformations Diagrams.* American Society for Metals (1977).
[7] Gundlach R. and Doane D. "Alloy Cast Irons". in *ASM Metals Handbook.* American Society for Metals (2003).
[8] Heine R.W. "A Model for Specific Volume and Expansion and Contraction Behavior of Solidifying Cooling Ductile and Gray Iron". *AFS Transactions* (1987).
[9] Kirkaldy J., Thomson B. and Baganis E. "Hardenability Concepts with Applications to Steel". in J.Kirkaldy and D.Doane (eds.) *AIME Transactions* (1978).
[10] Laird G., Gundlach R. and Rörig K. "Heat Treatment of High-Alloy AR Cast Irons". *Abrasion – Resistant Cast Iron Handbook.* American Society for Metals (1996).
[11] Lynch C.T. (ed.). *CRC Handbook of Materials Science- Vol.2:Metals, Composites and Refractory Materials* . CRC Press (1975).
[12] Sanchez Sarmiento G., X. Chen, J. Vega, G. Totten, R. Reynoldson, L. Huynh and L. Meekiso "A Comparison On Cooling Curve Analysis Using Inc-Phatran and Winprobe". *Proc. of 20th ASM Heat Treating Society Confererence,* (2000)
[13] Saunders N. "The Calculation of TTT and CCT diagrams for General Steels". *Thermotech Ltd., Surrey Technology Centre*, The Surrey Research Park, U.K. (2004).
[14] Stefanescue D. "Physical Properties of Cast Iron (Chapter 8)". in *Iron Castings Engineering Handbook.* American Society for Metals (1995).
[15] Wang D. "Thermophysical Property Data". Auburn Solidification Design Center. http://metalcasting.auburn.edu/data/data.html (2001).